IEEE Access
Multidisciplinary | Rapid Review | Open Access Journal

Received 12 August 2025, accepted 14 September 2025, date of publication 22 September 2025,
date of current version 26 September 2025.

Digital Object Identifier 10.1109/ACCESS.2025.3612846

RESEARCH ARTICLE

Optimizing Driver Position Using ANOVA and ANNs

MARCO FREDDI, CURZIO PAGLIARI, AND LEONARDO FRIZZIERO
Department of Industrial Engineering, University of Bologna, 40136 Bologna, Italy
Corresponding author: Marco Freddi (marco.freddi2@unibo.it)

ABSTRACT This study investigates how the optimal driving position is shaped by the forces acting on the driver and the performance requirements of an FSAE vehicle. Using a comprehensive dataset based on a parametric model, key SAE-standardized input variables are parameterized: the horizontal and vertical coordinates of the H-point, the horizontal distance between the AHP and H-point, the seatback angle, and the steering wheel position. The objective is to identify the ideal driving setup that balances vehicle performance with driver comfort. ANOVA is utilized to determine which of these ergonomic factors most significantly affect acceleration performance, while artificial neural networks provide a comparative method for validating results and predicting outcomes for new configurations. The novelty of this study lies in integrating driver positioning dynamics into performance optimization, providing a systematic approach to vehicle design before the CAD prototyping phase.

INDEX TERMS Vehicle dynamic, ANOVA, neural networks, ergonomics optimization, product architecture.

I. INTRODUCTION

The seated posture inside a vehicle significantly influences driver performance and control. The driver should safely operate the vehicle with adequate space and reachable controls [1]. Ergonomic principles are essential in optimizing posture. Tools like RAMSIS can simulate driver posture and optimize cabin layout based on human comfort evaluations. The integration of additive technologies in the seat design phases brings to study custom solutions using low-cost materials [2], [3], [4]. Adjustments such as moving the steering wheel and seat can enhance comfort for drivers of different heights and sitting positions as known in literature [5], [6].

However, many of these studies rely mainly on subjective or visual evaluations provided by participants, which limits their rigor and reliability [7]. Simulation-based methods can determine optimal driver seat adjustment ranges. Optimizing suspension parameters can improve ride comfort and reduce vertical acceleration at the driver's position, enhancing overall vehicle smoothness [8], [9]. Road type and driving style also significantly influence driver maneuvers. For this reason, studies in literature focus on the analysis of driver behavior in different road conditions [10]. Conducting ergonomic assessments and subjective evaluations validates optimization schemes and ensure driver comfort and safety [11]. Hybrid methods in literature combine approaches such as boundary manikin and special population to accommodate diverse drivers based on stature and weight, including pregnant women [1]. The driver's vehicle control significantly influences the behavior of the entire system, and specific events and patterns during cornering of a race car are analyzed to describe individual driving style [12]. Constructing musculoskeletal models based on biomechanical characteristics can help optimize the seating arrangement for different body types, enhancing comfort and reducing strain [13].

The integration of neural networks (ANNs) in these studies has often proved beneficial for optimizing vehicle design [14]. Both performance and safety topics are usually involved [15], together with ergonomic [16], and braking time tests [17]. The use of predictive numerical models is efficient if these can represent the real behavior of vehicles properly [18], [19], [20], [21], [22]. A major challenge in these tests is the high demand for large amounts of data [23]. The comparison with real-time sensors' data usually demonstrates

The associate editor coordinating the review of this manuscript and approving it for publication was Massimo Cafaro.

a good replication of the real behavior in virtual reality [24]. Response surface methodology (RSM), based on the analysis of variance (ANOVA), is often the best practice to map the behavior of the vehicle. This method allows for the recognition of influencing and not-influencing factors as a good decision model for designers [25]. Sometimes, RSM, analysis of variance and ANNs are used together. This integration usually works, as the RSM and ANNs results are estimated using different methods applied on the same database [26]. However, this integration to case specific studies related to drivers and passengers is still uncommon. Often only RSM is used avoiding multi-method approaches [27]. Another limitation is the frequent use of quarter-car models instead of full-vehicle models. Furthermore, there is also high dependency on the quality of data. The main contributions of this study attempt to overcome all the mentioned limitations. Using virtual models of the entire vehicle and the driver (Dempster approach), loads and vibrations can be predicted much earlier than experimental tests on real prototypes (as described in section II). Then, ANOVA and ANNs are used together and compared to predict the optimal position of the driver in the vehicle during the early stages of its design development (product architecture definition) [28]. Performances variation and critical driver's positions may be identified and corrected anticipating the issue in advanced phases of the project (section III). With this performance mapping, optimal configurations of vehicle architecture can be identified to conduct designers towards optimal choices.

II. PARAMETRIZATION OF THE DIGITAL TWIN AND DEFINITION OF VARIABLES

The aim of this study is to optimize the driving position of the driver in a Formula SAE (FSAE) monocoque applying mathematical approaches. Two analyses with different outputs are proposed. The first focuses on optimizing comfort and minimizing driver loads during acceleration. To maximize the pitch effect (and associated loads), traction is applied to the rear axle, while braking is assigned to the front axle. The second analysis uses the same inputs but is aimed at optimizing the acceleration performance. The minimization of the time to reach a speed of 50 km/h from a standstill is the objective function in the second case. The motor torque law (50 Nm from engine, 150 Nm on wheels) is the same in all the simulations. In other words, the driver is doing the same thing every time. This choice is necessary to isolate the effect of vehicle-referenced inputs on changes in output forces. Designers principally need to identify the most significant factors reaching an optimal configuration.

Six variables are selected and systematically varied to generate the dataset used for training the neural network in this study. However, the method is generically applicable to any field and case study [29]. These variables, along with their respective ranges, are: horizontal position of H-point (z_{HP}, in range [500; 900 mm] with reference to the front axle), vertical position of H-point (y_{HP}, [−100; 50 mm]), horizontal distance between AHP (Acceleration Heel Point) and H-point (L_0, [650; 850 mm]), backrest tilt (a, [30; 70 degree]), horizontal position of the steering wheel (z_{SW}, [−150; 0 mm]) and vertical position of the steering wheel (y_{SW}, [−150; 0 mm]). Fig.1 will be useful for readers to visualize the parameterization discussed in the digital twin.

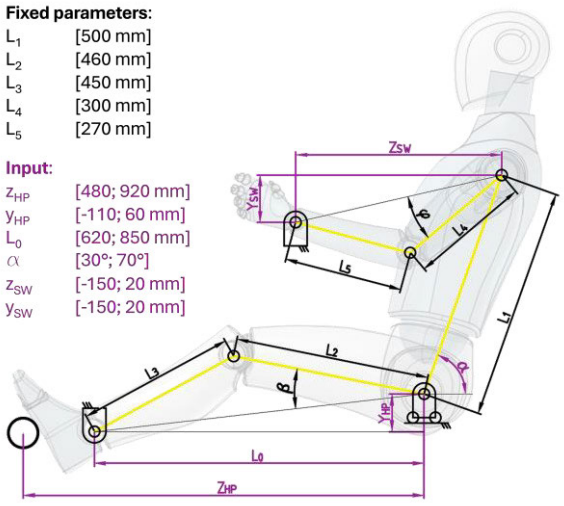

FIGURE 1. List of the input factors and mannequin schematization.

The digital twin used in this study is a simplified numerical model rather than a classic CAD model, which is a key aspect of our approach. This allows for rapid and efficient analysis of a wide range of configurations in the very early design stages, a significant departure from methods that require full-scale CAD mockups [30].

A virtual driver model is incorporated into the vehicle to estimate realistic weights and loads. It represents an 85 kg subject based on the Dempster anthropometric model. It is divided into multiple segments, each with defined weights and moments of inertia, and it can represent the 95th percentile of the population. The anthropometric standards for the 95th percentile dummy are defined by various regulatory bodies and research institutions. Key references include SAE International, which provides vehicle ergonomics standards such as SAE J826 (for H-point machine) and SAE J4002 (driver selected seat position); ISO (International Organization for Standardization), which publishes ISO 7250 for standardized anthropometric data; and NHTSA (National Highway Traffic Safety Administration), which establishes specifications for crash test dummies like the Hybrid III 95th percentile male dummy. Some references such as Manouvrier's tables are used for the lengths of bone segments. The study does not reach this level of detail and follows the already mentioned SAE J826 standards and SAE J1100 for motor vehicle dimensions [30], [31]. In the model proposed in Fig.1, the closure of the chain representative of the mannequin must be respected. To understand the degrees of freedom of the model, Grubler's formula can be used. Two different possible initial schematizations application-dependent are proposed in Fig.2 and Fig.3.

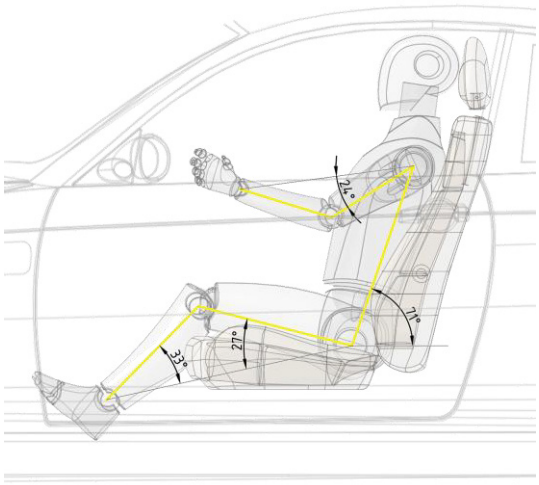

FIGURE 2. Seating configuration for road cars.

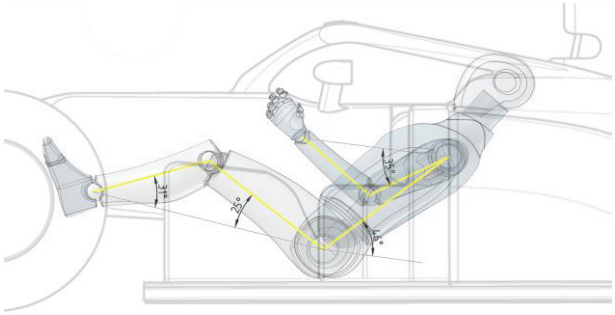

FIGURE 3. Seating configuration for sport cars.

The rigid driver assembly is constrained to the chassis by two fixed hinges at the ankles and wrists. The feet and hands are not included in the model. It is intuitive and reasonable to assume that during acceleration, the foot rotates around an instantaneous center of rotation located at the ankle. Similarly, the wrist allows relative rotation between the hand (fixed on the steering wheel) and the forearm (Fig. 3). A sliding joint is placed at the H-point.

Dempster's model consists of 11 elements. The head is not really involved because the upper-right hinge is positioned at the shoulder. The right arms and legs are symmetrically positioned like the left ones, leaving five rigid segments. Each hinge removes two degrees of freedom (horizontal and vertical translation), while the sliding joint at the H-point, connected to the chassis by two rods, removes three degrees of freedom. The final degrees of freedom of the full assembly are:

$$DOF = 5 \cdot 3 - 5 \cdot 2 - 1 \cdot 3 = 2 \tag{1}$$

Two variables are sufficient to uniquely represent the kinematic chain (i.e., the driver's position). Just as in a vehicle, these can be the seatback inclination and the horizontal position of the seat relative to the pedals (denoted as a and L_0 in Fig.1).

The proposed model increases complexity by allowing the chain to open at the steering wheel. It is free to be adjusted both horizontally and vertically, as its position is not yet defined in the vehicle design.

Two variables, z_{SW} and y_{SW}, are added to the model. Finally, the vertical position of the H-point is added to the model (y_{HP}) together with the positioning of the entire structure in relation to the front axle of the vehicle (z_{HP}). There are six total variables. The other geometric quantities used to close the chain in the are based on trigonometry formulas. Thanks to the Carnot-Al-Kashi cosine theorem, it is possible to calculate the angles b and ϕ. In fact, according to (2):

$$\begin{aligned} L_3^2 &= \left(L_0^2 + y_{HP}^2\right) + L_2^2 - 2L_2\sqrt{L_0^2 + y_{HP}^2}\cos\beta \\ &\rightarrow \beta = \cos^{-1}\left(\frac{L_2^2 - L_3^2 + L_0^2 + y_{HP}^2}{2L_2\sqrt{L_0^2 + y_{HP}^2}}\right) \end{aligned} \tag{2}$$

$\sqrt{L_0^2 + y_{HP}^2}$ is the distance calculated by the Pythagorean theorem between the AHP and H-point. Similarly, (3):

$$\varphi = \cos^{-1}\left(\frac{L_4^2 - L_5^2 + (z_{SW} - z_{SH})^2 + (y_{SW} - y_{SH})^2}{2L_4\sqrt{(z_{SW} - z_{SH})^2 + (y_{SW} - y_{SH})^2}}\right) \tag{3}$$

Quantities $(z_{SW} - z_{SH})$ e $(y_{SW} - y_{SH})$ are the horizontal and vertical distances between the driver's wrist (on the steering wheel) and the shoulder. Observing Fig.1 it is possible to guess (4) and (5):

$$z_{SH} = z_{HP} + L_1\cos\alpha \tag{4}$$

$$y_{SH} = y_{HP} + L_1\sin\alpha \tag{5}$$

Imposing the equations in the setup ensures that varying the six inputs will respect the conservation of the lengths of the dummy elements (the software used is Nx Motion).

A. ANALYSIS OF VARIANCE AND THE MOST INFLUENTIAL VARIABLES

When the p-value of a generic input factor is close to 0 there is statistical relevance. That input has a real influence on the analyzed output. In general, CAD optimization tools or neural networks cannot bring this information as they are generally used to identify optimal solutions by designers in industry. The p-value quantifies the probability of observing an effect equal to or more extreme than the one obtained, if the null hypothesis (H_0) is true. It is calculated as:

$$p = P\left(|T| > t_{obs}\right) \tag{6}$$

T is the t-statistic distributed according to the t-student or normal distribution of the sampling, whereas t_{obs} is the value of the calculated t-statistic.

If $p < \alpha$ (significance level, in our case $\alpha = 0.05$) and close to 0 there is in fact significance in the determination of outputs.

At the end of RSM or ANNs models training, R^2 coefficient can be evaluated making predictions on the dataset elements and new factors' combinations. The adjusted R^2 is:

$$R^2_{\text{adj}} = 1 - \frac{\frac{SS_E}{n-p}}{\frac{SS_T}{n-1}} = 1 - \left(\frac{n-1}{n-p}\right)\left(1 - R^2\right) \tag{7}$$

In the formula, SS_E is the error sum of squares and SS_T is the total sum of squares. In general, the adjusted R^2 statistics will not always increase as variables are added to the model. If unnecessary terms are added, its value will decrease in general. This term is good to predict the model fitting with the database.

Residual analysis, then, should demonstrate that they are small and they follow a random distribution. The regression equations derived from the model can then be utilized to predict future outputs. If the response is well modeled by a linear function of the independent variables, then the approximating function is the first-order model:

$$y = \beta_0 + \beta_1 x_1 + \beta_2 x_2 + \cdots + \beta_k x_k + \epsilon \tag{8}$$

If there is curvature in the system, then a polynomial of higher degree must be used, such as the second-order model:

$$y = \beta_0 + \sum_{i=1}^{k} \beta_i x_i + \sum_{i=1}^{k} \beta_{ii} x_i^2 + \sum_{i<j} \beta_{ij} x_i x_j + \epsilon \tag{9}$$

In these equations, the terms b are scalar coefficients derived from the DOE. Terms in x are the input variables taken individually or combined. The constant term ϵ complete the polynomial regression. Higher-order models can be used to improve the fitting of the solution.

The minimum number of tests to be performed depends on N and O (number of factors and order of the polynomial regression model). This is the number of spatial points necessary to define the only hypersurface passing through them. If the regression analysis is mono-variable and linear (N=O=1), a straight line is theoretically sufficient as it is definable only if at least two of its points are given. For a plane (N=2, O=1) 3 points (3 tests) are needed. In general, for 1st order models, $N + 1$ tests are required. Analysis of higher order statistics requires a minimum number of tests equal to:

$$\binom{N+O}{N} = \frac{(N+O)!}{N! \cdot O!} \tag{10}$$

The number of outputs has no influence. In this study, with $N = 8$ and $O = 2$, 45 tests were needed. However, as it is true that a statistical model needs to be validated, 3,4, or 5 times this value of tests can be performed. Evaluating the R^2_{adj} and R^2_{pred} coefficients can then demonstrate if there is overfitting or not. If a 2nd order is chosen, it is sure that overfitting will not happen as the model will have constant curvature (the 2nd order gradient will be constant). For this reason, the author's advice is to avoid too high O values (this is also to avoid too large number of required tests).

Finally, to find the best input configuration, the identification of a max, min or minimax (saddle) point is conducted. This point, if it exists, will be the set of $x_1, x_2, \ldots, x_n$ for which the partial derivatives:

$$\frac{\partial \hat{y}}{dx_1} = \frac{\partial \hat{y}}{\partial x_2} = \ldots = \frac{\partial \hat{y}}{\partial x_k} = 0 \tag{11}$$

a stationary point. The stationary point could represent a point of maximum response, a point of minimum response, or a saddle point. If the optimal point is not in the domain new tests could be performed following the curve trend.

B. NEURAL NETWORK SETUP

The definition of an optimal setup for a neural network remains a general challenging task. In this work, the neural network architecture was designed with six input neurons, corresponding to the six input variables under analysis, and one output neuron to predict the target metric. A range of architectures was systematically tested by adjusting the number of hidden layers (from one to three) and neurons per layer (between three and eight) to identify the most effective configuration. The selection criteria included minimization of the loss function and maximization of both predicted and adjusted R^2 values (Matlab is useful for this type of research, using Deep Learning toolbox). After comparative evaluation, the configuration delivering the best performance consisted of two hidden layers, each containing six neurons, as shown in Fig.4.

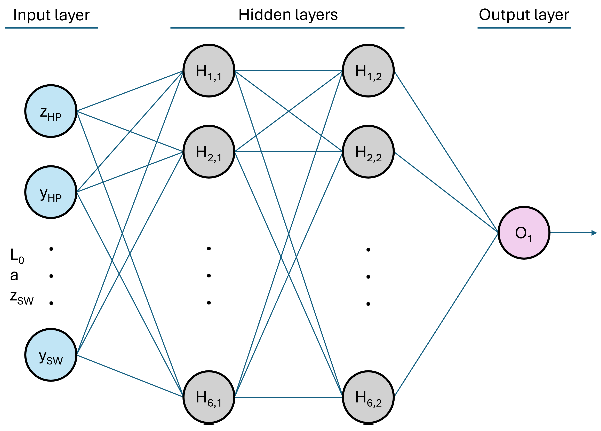

FIGURE 4. NN scheme used for training in this study.

The neural network developed for this study is a Multilayer Perceptron (MLP) with a feedforward architecture, consisting of an input layer, two fully connected hidden layers, and a single output layer. A small excerpt of the database used is in Fig.5.

The hidden layers utilize Rectified Linear Unit (ReLU) activation functions, which were selected due to their superior performance in this case compared to sigmoid and tanh,

Dataset (first specimens)

z_{HP}	y_{HP}	l_0	α	z_{SW}	y_{SW}	$F_{SHOULDER}$	F_{ELBOW}
766.667	0.000	783.333	56.667	-50.000	-50.000	261.766	237.630
633.333	0.000	716.667	70.000	0.000	-50.000	271.784	203.423
900.000	-50.000	716.667	30.000	-50.000	0.000	179.919	303.408
766.667	50.000	850.000	43.333	-100.000	-50.000	273.915	280.233
633.333	0.000	850.000	70.000	-150.000	-100.000	290.112	311.284

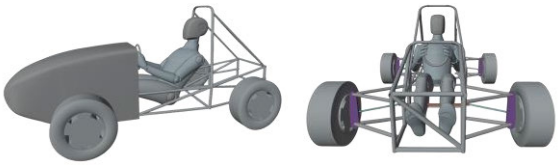

FIGURE 5. First rows of the dataset generated by the simulations.

particularly when applied to normalized data in the [0; 1] range. Designed specifically for regression tasks, the network is trained over 450 epochs with a batch size of 45, using the Adaptive Moment Estimation (Adam) optimizer, known for its robustness in handling non-stationary objectives and adaptive learning rates. The learning rate has been set at 0.01. Validation was performed every 25 iterations, and the overall training progress was monitored through MATLAB's built-in visualization tools. Explicit regularization techniques are not used as the use of simple architecture reduces the risk of overfitting.

III. RESULTS

A total of 150 simulations is performed (using Nx Motion), by varying the 6 input parameters randomly in the domain. The 150 tests are generated using a random sampling approach within the domains defined for the six input variables. In this specific case, this method is preferred over a factorial design to ensure a larger, less structured coverage of parameter space. This approach is particularly effective for training neural networks, as it reduces the risk of bias from a predefined grid of test points, allowing the model to learn patterns even from less intuitive input combinations.

The decision to limit the study to longitudinal acceleration was deliberate, motivated by two main reasons. Our primary objective was to analyze the impact of the driver's position during the most intense dynamic phases typical of a competition. Acceleration is one of the most extreme conditions and represents a critical case for the evaluation of the forces acting on the driver's body. Although the full model of the vehicle is used, focusing on a single dynamic condition isolates and analyzes the influence of ergonomic parameters more deeply without the addition of unnecessary variables and complexities resulting from other maneuvers (e.g. high-speed cornering or braking, or different case studies that readers may try to develop).

Maximum force values on the shoulders, pelvis, head and the time (t^*) taken by the vehicle to accelerate from 0 to 50 km/h are measured at the end of all tests. The minimum t^* recorded is 3.530 seconds, while the maximum is approximately 3.558 seconds. This shows that the dummy's position had no real effect on the vehicle's acceleration performance.

Highly significant results are obtained on the study of the forces. Table 1 schematizes the first ANOVA of the study. The most influential variables are D, A, B in the diagram, i.e. a and the coordinates of the H-point. The other most influential terms (1st and 2nd order) are in Fig.6. As shown in that figure, the adjusted and predicted R^2 coefficients are 96.91% and 95.34%, respectively, demonstrating the high reliability of the RSM model.

TABLE 1. ANOVA related to shoulder force.

Source	DF	Adj SS	Adj MS	F-Value	P-Value
Model	12	42163.3	3513.61	155.07	0.000
Linear	6	13778.1	2296.34	101.35	0.000
z_{HP}	1	4333.3	4333.32	191.25	0.000
y_{HP}	1	1073.3	1073.31	47.37	0.000
l_0	1	668.0	668.02	29.48	0.000
a	1	8879.6	8879.64	391.90	0.000
z_{SW}	1	613.4	613.42	27.07	0.000
y_{SW}	1	64.5	64.53	2.85	0.098
Square	2	1283.1	641.56	28.32	0.000
l_0*l_0	1	141.7	141.73	6.26	0.016
a*a	1	929.5	929.50	41.02	0.000
2-Way Interaction	4	1831.5	457.87	20.21	0.000
z_{HP}*a	1	764.1	764.07	33.72	0.000
y_{HP}*l_0	1	529.7	529.72	23.38	0.000
l_0*z_{SW}	1	57.6	57.57	2.54	0.118
z_{SW}*y_{SW}	1	14.9	14.93	0.66	0.421
Error	47	1064.9	22.66		
Lack-of-Fit	44	1064.9	24.20	*	*
Pure Error	3	0.0	0.0		
Total	59	43228.2			

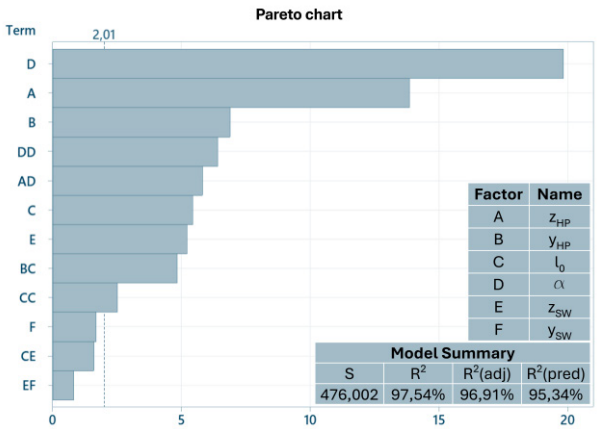

FIGURE 6. Pareto chart related to shoulder force ANOVA with Pearson coefficients.

The results obtained for the forces on the pelvis are similar. The most influential variables in that case are A, C, D, AC, DE, CC, AA, CD, F, BD, EE, CF, AF all above the significance level. The z position of the H-point wins,

followed by L_0 and a. In this case adjusted and predicted R^2 coefficients are 99.48% and 98.93%. Regarding the force on the neck-head joint, the most influential variables are in that case A, AD, AA, B, DD, AF, BC, DE, D, CC, AC, BB, F, DF, FF all above the significance level. The z position of the H-point wins, followed by the mixed term composed of the same z_{HP} and a and the second-order term in z_{HP}. Then y_{HP} follows. In this case, the adjusted and predicted R^2 coefficients are 99.14% and 98.14%. All three analyses of variance are highly accurate based on the evaluation of the Pearson R^2 coefficients.

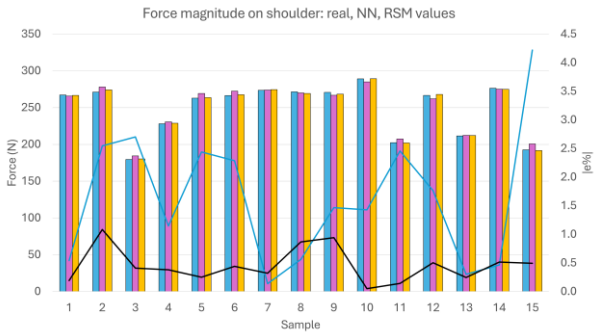

FIGURE 7. Comparison of RSM and NN predictions on real shoulder load data.

To evaluate the predictive ability and generalization of the models on configurations not previously seen, 15 new tests are performed. The results of these 15 tests are used for the comparisons presented in Figures 7, 8, and 9. The graph appears saturated. For each sample, the three result columns (real values, RSM predictions, NN predictions) have nearly the same height. This indicates that the predictions from both models are consistent and closely match the simulated values. For the shoulder tests, the neural network yields an absolute mean error |e%| of 1.173%, while the RSM produces an error of 0.511%. Improved network training could easily reduce this error threshold. Similarly, Fig.8 presents comparative data on the loads applied to the driver's pelvis.

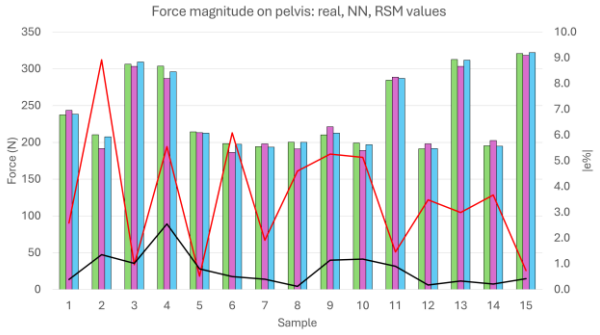

FIGURE 8. Comparison of RSM and NN predictions on real pelvis load data.

In this case, the absolute mean error of the RSM calculated on the dataset predictions is 0.66%, while that of the neural network (NN) is 2.486%. Finally, Fig.9 presents the comparative analysis of the loads acting on the driver's head. The highest recorded force values are due to the jerking motion caused by vehicle acceleration and braking. In these cases, the head moves backward during acceleration and forward during braking.

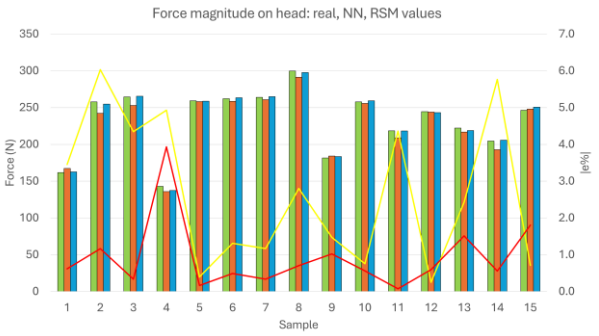

FIGURE 9. Comparison of RSM and NN predictions on real head load data.

Despite the system's complexity and the number of interacting variables, both NN and RSM demonstrate strong predictive capabilities, making them reliable tools during the early stages of vehicle design. In particular, the NN shows excellent generalization on previously unseen data, with minimal percentage errors (|e%|), as indicated in the results table. The difference in errors is a demonstration of robustness. The slight discrepancy in errors does not indicate poor NN performance. On the contrary, the consistency of the forecasts between the two models, with different methodologies and architectures, strengthens the thesis. The 2.5% error of the ANN is within an acceptable range for the preliminary design phase, where the goal is to identify trends and not achieve the accuracy of a detailed physical model. Both models successfully predict the biomechanical loads and performance of the vehicle.

Beyond model validation, a key outcome of this study is the ability to determine the optimal input conditions that yield the best-performing vehicle configuration in terms of acceleration. This approach effectively delivers a functional input-output map, enabling designers to make informed decisions when laying out the vehicle architecture. Although the analysis focused on the acceleration phase, the methodology is easily extendable to other performance criteria. The resulting optimal setup derived from this process is detailed in Table 2.

TABLE 2. Design parameters for the driver's seat in the optimal configuration.

z_{HP}	y_{HP}	L_0	α	z_{SW}	y_{SW}
747.4 mm	-22.4 mm	620 mm	39.7°	-26.3 mm	-68.4 mm

In practical scenarios, certain parameters may be constrained by design requirements or regulatory standards. In such cases, the designer can lock those fixed values and

perform a targeted optimization on the remaining variables, taking advantage of the neural network's ability to predict outcomes efficiently.

Moreover, the trained ANN model from this study holds potential as a modular component within a broader predictive framework. It can be combined with other specialized networks, each trained under different testing conditions or vehicle configurations (such as varying suspension setups, tire types, or weight distributions based on competition rules), to build a more comprehensive design support system.

Although this study focused on the virtual design phase, it is our intention to integrate validation with experimental data in future work. We plan to conduct the following tests soon. We will use an FSAE vehicle equipped with force sensors and accelerometers to measure biomechanical forces under real driving conditions. We will use a professional driving simulator to collect data on the behavior of the drivers and compare them with the predictions of our model.

Furthermore, the virtual mannequin used, though compliant with standards, is a rigid body model. It doesn't account for biological variability, the driver's active muscle response, or fatigue. These factors could alter the biomechanical forces in real-world scenarios. The conclusions are based on a digital twin which, despite its detail, is a simplification of reality. Although the correlation between the ANN and RSM models is high, final validation of the results with real-world data remains a necessary step to confirm their validity. However, the general applicability of the method to other case studies and different design contexts represents its main strength.

IV. CONCLUSION

By employing a digital twin of the vehicle and a biomechanically realistic Dempster mannequin, six ergonomic parameters were systematically varied to assess their influence on both driver load and vehicle performance during acceleration. The results showed that while the driver's position had a negligible effect on pure acceleration times, it significantly impacted the biomechanical loads experienced by the shoulders, pelvis, and head. The ANOVA provided clear identification of the most influential factors, while the ANN proved highly effective in generalizing predictions to new, unseen configurations. This dual approach enhances the robustness of the design recommendations.

Future work will extend this method to other driving scenarios, such as cornering and braking, and integrate it into a real-time design decision support system. Limitations related to fixed component positions and regulatory constraints can be addressed by locking certain parameters during optimization. Overall, this framework represents a scalable, adaptable, and practical contribution to the ergonomic and performance-based design of modern vehicles.

REFERENCES

[1] J. Gragg, J. Yang, and B. Howard, "Hybrid method for driver accommodation using optimization-based digital human models," *Comput.-Aided Des.*, vol. 44, no. 1, pp. 29–39, Jan. 2012, doi: 10.1016/j.cad.2010.11.009.

[2] A. Bacciaglia, A. Liverani, and A. Ceruti, "Efficient part orientation algorithm for additive manufacturing in industrial applications," *Int. J. Adv. Manuf. Technol.*, vol. 133, nos. 11–12, pp. 5443–5462, Aug. 2024, doi: 10.1007/s00170-024-14039-z.

[3] A. Bacciaglia and A. Ceruti, "Efficient toolpath planning for collaborative material extrusion machines," *Rapid Prototyping J.*, vol. 29, no. 9, pp. 1814–1828, Oct. 2023, doi: 10.1108/rpj-09-2022-0320.

[4] A. Montalti, G. Galiè, E. Pignatelli, and A. Liverani, "Enhancing surface roughness of material extrusion additive manufacturing components via an innovative ironing process," *Virtual Phys. Prototyping*, vol. 19, no. 1, Dec. 2024, doi: 10.1080/17452759.2024.2401929.

[5] S. Li, Z. Zhang, and W. Han, "Optimization of driver cabin human factors design for sweeper truck based on RAMSIS: Enhancing driver comfort and safety," in *Proc. Int. Conf. Hum.-Comput. Interact.*, 2023, pp. 96–111, doi: 10.1007/978-3-031-48047-8_6.

[6] A. B. Rathod and R. T. Vyavhare, "Optimization of truck driver cab ergonomic for commercial truck based on ramsis: Enhancing driver comfort and safety," *Int. J. Intell. Transp. Syst. Res.*, vol. 22, no. 3, pp. 603–613, Dec. 2024, doi: 10.1007/s13177-024-00419-y.

[7] H.-J. Wirsching and M. Fleischer, "Ergonomic simulation in automated vehicles using RAMSIS," *Zeitschrift für Arbeitswissenschaft*, vol. 76, no. 4, pp. 478–488, Nov. 2022, doi: 10.1007/s41449-022-00334-6.

[8] T. Zhou, L. Wang, T. Wang, and L. Yuan, "Vertical dynamics optimization of a light bus suspension system," *Zhendong Yu Chongji/J. Vibrat. Shock*, vol. 42, no. 14, pp. 131–137, Jan. 2023.

[9] L. R. C. Drehmer, H. M. Gomes, and W. J. Paucar Casas, "An interval-based multi-objective robust design optimization for vehicle dynamics," *Mech. Based Design Struct. Mach.*, vol. 51, no. 12, pp. 7076–7101, Dec. 2023, doi: 10.1080/15397734.2022.2088557.

[10] R. Jurecki, T. Stańczyk, and M. Ziubiński, "Analysis of the structure of driver maneuvers in different road conditions," *Energies*, vol. 15, no. 19, p. 7073, Sep. 2022, doi: 10.3390/en15197073.

[11] H. R. Lourenço and M. Ackermann, "Passenger vehicle driver's lower limbs ergonomics through the development of biomechanical models," SAE Tech. Papers 2015-36-0205, 2015, doi: 10.4271/2015-36-0205.

[12] L. Wörle, M. Graf, and A. Eichberger, "Objective metrics for control inputs of racecar drivers," in *Proc. FISITA World Automotive Congr.*, 2018.

[13] M. Li, Z. Gao, F. Gao, and T. Zhang, "Research on comfortable driving posture of car drivers based on muscle biomechanics," *Proc. Inst. Mech. Eng., D, J. Automobile Eng.*, vol. 236, nos. 10–11, pp. 2230–2243, Sep. 2022, doi: 10.1177/09544070211055281.

[14] A. Baicoianu, P. Stanoiu, M. Velea, and C. Husar, "A machine learning proposal for condition monitoring of vehicle suspension," in *Proc. Int. Conf. Innov. Intell. Syst. Appl. (INISTA)*, Aug. 2022, pp. 1–5, doi: 10.1109/INISTA55318.2022.9894160.

[15] F. Terrosi, L. Strigini, and A. Bondavalli, "Impact of machine learning on safety monitors," in *Computer Safety, Reliability, and Security (SAFECOMP)* (Lecture Notes in Computer Science), vol. 13414, M. Trapp, F. Saglietti, M. Spisländer, and F. Bitsch, Eds., Cham, Switzerland: Springer, 2022, doi: 10.1007/978-3-031-14835-4_9.

[16] X. Zhou, Z. Miao, M. Yuan, K. Li, H. Guo, X. Lin, Y. Zeng, R. Tu, and J. Zhong, "Dual-phase prediction model of passenger thermal sensation using facial thermal imaging and environmental factors," *Case Stud. Thermal Eng.*, vol. 58, Jun. 2024, Art. no. 104439, doi: 10.1016/j.csite.2024.104439.

[17] H. Zhang, S. Ono, and H. Kawasaki, "Braking detection and prediction with inter-vehicle distance estimated from driving videos," *Int. J. Intell. Transp. Syst. Res.*, vol. 23, no. 1, pp. 281–289, Nov. 2024, doi: 10.1007/s13177-024-00449-6.

[18] J. Gao, X. Zhang, and X. Yu, "A design optimization process of improving the automotive subframe dynamic stiffness using tuned rubber mass damper," *SAE Int. J. Vehicle Dyn., Stability, NVH*, vol. 8, no. 2, pp. 253–263, Apr. 2024, doi: 10.4271/10-08-02-0014.

[19] A. Aksjonov and V. Kyrki, "A safety-critical decision-making and control framework combining machine-learning-based and rule-based algorithms," *SAE Int. J. Vehicle Dyn., Stability, NVH*, vol. 7, no. 3, pp. 287–299, Jun. 2023, doi: 10.4271/10-07-03-0018.

[20] B. B. Zheng, Y. Guo, L. Xiao, D. Zheng, G. Li, W.-B. Shangguan, and S. Rakheja, "Optimization of idle vibration characteristics of powertrain mounting system," *SAE Int. J. Vehicle Dyn., Stability, NVH*, vol. 8, no. 3, pp. 329–345, May 2024, doi: 10.4271/10-08-03-0018.

[21] M. M. H. Kolta, N. A. Mansour, M. Lashin, and A. M. A. Soliman, "Optimal layout of suspension system employing mechatronic inerter for comfort enhancement based on structure-immittance approach," *SAE Int. J. Vehicle Dyn., Stability, NVH*, vol. 8, no. 3, pp. 409–425, Jul. 2024, doi: 10.4271/10-08-03-0023.

[22] R. Marotta, S. Strano, M. Terzo, and C. Tordela, "Multi-output physically analyzed neural network for the prediction of tire–road interaction forces," *SAE Int. J. Vehicle Dyn., Stability, NVH*, vol. 8, no. 2, pp. 285–308, May 2024, doi: 10.4271/10-08-02-0016.

[23] G. Valente, M. Perrelli, R. Adduci, F. Cosco, R. Bossio, and D. Mundo, "Hybrid physics-based and data-driven modelling for vehicle dynamics simulation," in *Mechanisms and Machine Science*. Cham, Switzerland: Springer, 2024, pp. 398–406, doi: 10.1007/978-3-031-64569-3_45.

[24] G. Riva, S. Formentin, M. Corno, and S. M. Savaresi, "Experimental assessment of neural networks for tire-road force estimation," in *Proc. IEEE Conf. Control Technol. Appl. (CCTA)*, Aug. 2022, pp. 658–663, doi: 10.1109/CCTA49430.2022.9966175.

[25] F. Hegedüs, P. Gáspár, and T. Bécsi, "Fast motion model of road vehicles with artificial neural networks," *Electronics*, vol. 10, no. 8, p. 928, Apr. 2021, doi: 10.3390/electronics10080928.

[26] J. Kasac, J. Deur, B. Novakovic, I. V. Kolmanovsky, and F. Assadian, "A conjugate gradient-based BPTT-like optimal control algorithm with vehicle dynamics control application," *IEEE Trans. Control Syst. Technol.*, vol. 19, no. 6, pp. 1587–1595, Nov. 2011, doi: 10.1109/TCST.2010.2084088.

[27] A. R. Mohammed, Z. Saleh, A. M. Aldabbagh, and A. Al Hanbali, "Multi-objective ergonomics design model optimization for micro electric cars via response surface methodology," *Discover Appl. Sci.*, vol. 6, no. 10, Oct. 2024, doi: 10.1007/s42452-024-06219-z.

[28] L. Frizziero, G. Galiè, C. Leon-Cardenas, M. De Santis, M. S. Losito, and A. Tomaiuolo, "Design of a concept vehicle for future-oriented urban mobility using design-driven methodologies," *Heliyon*, vol. 9, no. 3, Mar. 2023, Art. no. e14462, doi: 10.1016/j.heliyon.2023.e14462.

[29] D. C. Montgomery, *Design and Analysis of Experiments*. Hoboken, NJ, USA: Wiley, 2013.

[30] R. J. Mau and P. J. Venhovens, "Development of a consistent continuum of the dimensional parameters of a vehicle for optimization and simulation," *Proc. Inst. Mech. Eng., D, J. Automobile Eng.*, vol. 228, no. 6, pp. 591–603, May 2014, doi: 10.1177/0954407013497195.

[31] M. P. Reed, R. W. Roe, M. A. Manary, C. A. C. Flannagan, and L. W. Schneider, "New concepts in vehicle interior design using ASPECT," Univ. Michigan Transp. Res. Inst., USA, Tech. Rep., 1999.

MARCO FREDDI is currently pursuing the Ph.D. degree with UNIBO.

He performs CAD modeling/design and applications in reverse-engineering methods. He works in multiple contexts, such as purely mechanical, medical/health field, and car design. He has been involved in virtual reconstruction and redesign/optimization of models of components, such as connecting rods, pistons, cylinder heads, crankshafts, gears, and hydraulic pumps whose main objective is light weighting; laser scanning; re-design/quality control of instruments used in the surgical-orthopedic field, such as femoral compression plates and cutting masks; and the design in the nautical field of boats, such as a bi-hull racing catamaran. He is the author or co-author of several publications.

CURZIO PAGLIARI received the master's degree in mechanical engineering. He is currently pursuing the Ph.D. degree in automotive engineering for intelligent mobility with the University of Bologna. His master's thesis dedicated to the development of a sports coupe concept car in the field of automotive and product development, partially conducted at Lawrence Technological University, USA. He has interdisciplinary expertise in industrial engineering and additive manufacturing. He focused on research and development in innovative automotive applications. He was a Teaching Assistant in engineering drawing and methods and a Chapter Officer for IEOM, promoting engineering knowledge dissemination. During an internship with the Department of Industrial Engineering, University of Bologna, in collaboration with the Rizzoli Orthopedic Institute, he applied CAD simulations to complex pediatric orthopedic procedures, and gaining direct experience in surface modeling and complex models.

LEONARDO FRIZZIERO received the Ph.D. degree. He is an Associate Professor with UNIBO. In the academic field, he promotes scientific topics related to design and methods of industrial engineering (2-D CAD, 3-D CAD, Advanced Design, QFD, TRIZ, DFSS, DFD, and DFA). In 2005, he was hired by Ferrari Spa, as a Team Planner for new Ferrari car projects, coordinating methodologies, timelines, and costs. In 2009, he returned to the university, collaborated with the Research Group on Design and Methods of Industrial Engineering, and became a Junior Researcher with the Department of Industrial Engineering (DIN), A.M.S. University of Bologna, in February 2013. He has engaged in teaching and research activities, participating in various regional, national, and international competitive projects. Since 2018, he has been a Senior Researcher. In 2017, he received the qualification for an Associate Professor in design and methods of industrial engineering (ING-IND/15), assuming this role in 2021 with the Department of Industrial Engineering. Prior to his academic career, he held significant responsibilities in various industrial sectors. He is the author or co-author of more than 150 publications on topics related to design and methods in industrial engineering, industrial and car design, DFSS, SDE, CAD, TRIZ, QFD, Fuzzy Logic, and GA. Since January 2020, he has been a member of the Doctoral Board in Mechanics and Advanced Engineering Sciences (DIMSAI).